Enhancement mechanisms for optical forces in integrated optics

M. L. Povinelli[(a)], M. Lončar[(b)], E. J. Smythe[(b)], M. Ibanescu[(c)], S. G. Johnson[(d)], F. Capasso[(b)], and J. D. Joannopoulos[(c)]

[(a)]Ginzton Laboratory, Stanford University, Stanford CA 94305
[(b)]Division of Engineering and Applied Sciences, Harvard University, Cambridge MA 02138
[(c)]Department of Physics and Center for Material Sciences and Engineering, Massachusetts Insitute of Technology, Cambridge MA 02139
[(d)]Department of Mathematics, Massachusetts Institute of Technology, Cambridge MA 02139

ABSTRACT

We investigate the extension of optical micromanipulation to integrated optics. In particular, we consider whether propagating light signals can cause mechanical reconfiguration of a device. While such forces are intrinsically weak, we predict theoretically that significant displacements can be achieved using various enhancement mechanisms. These include the use of high-index materials, high-Q (cavity quality factor) enhancement, and slow light in photonic crystals. Silicon optical waveguides have a considerable refractive index contrast with the surrounding air, with a ratio of roughly 3.45/1 at optical communications wavelengths. We show that the strong confinement of light to silicon magnifies optical forces arising from overlap in the guided modes of neighboring waveguides. Silica microsphere resonators are known to have extremely high cavity quality factors, in excess of 10^8. We show that the quality factor of the resonator magnifies the optical force due to modal overlap between two neighboring spheres. Thirdly, we investigate slow-light enhancement of optical forces using photonic-crystal devices. We show that slow-light velocities give rise to larger forces for the same amount of signal power, enhancing optomechanical coupling effects. In addition to being of fundamental interest, our work suggests that optical manipulation may ultimately provide a route to all-optical conformational control and switching.

1. INTRODUCTION

We are interested in optical forces in the context of microphotonic devices. While a great deal of knowledge exists concerning the use of optical forces (or radiation pressure) to trap atoms and dielectric particles, these applications typically employ external laser beams for the manipulation of matter. In contrast, we are interested in the circumstances under which light propagating within integrated, micro- or nano-photonic devices can be used to exert optical forces on the device, resulting in mechanical reconfiguration. Since the optical power of these signals is weak (typically on the order of mW), it is necessary to investigate mechanisms for enhancing the optical force to observable and potentially useful levels. In this paper, we describe our recent work in this area,[1–3] presenting sample device geometries that illustrate the principles of high-index, high-Q (quality factor), and slow-light enhancement of optical forces.

Our general numerical method for the calculation of optical forces in guided-wave structures employs the Maxwell stress-tensor formalism.[4,5] The time-averaged force at any given frequency can be calculated from the eigenmode solutions of the dielectric structure as

$$F_\alpha = \oint_S da \sum_\beta \frac{1}{8\pi} \mathrm{Re}\left[\epsilon E_\alpha^* E_\beta - \frac{1}{2}\delta_{\alpha\beta}\epsilon |E|^2 + \mu H_\alpha^* H_\beta - \frac{1}{2}\delta_{\alpha\beta}\mu |H|^2\right] n_\beta. \quad (1)$$

where the integral is taken over a surface S enclosing the object on which the force is calculated, and $\hat{n}$is the outward normal to this surface. The stress tensor expression is unambiguous provided that the integration surface

Optical Trapping and Optical Micromanipulation III, edited by Kishan Dholakia, Gabriel C. Spalding, Proc. of SPIE Vol. 6326, 632609, (2006) · 0277-786X/06/$15 · doi: 10.1117/12.681066

lies completely in the air. Using symmetry considerations, this expression can often be further simplified. To calculate the eigenmode fields E and H of the structure, we typically use the plane-wave expansion method.[6]

Alternatively, we have shown[1–3] that for guided-wave structures, the force between two objects can be calculated from the derivative of the eigenmode energy with respect to separation. That is,

$$F = -\frac{1}{\omega}\left.\frac{\partial\omega}{\partial\xi}\right|_{\mathbf{k}} U_{\text{field}} \tag{2}$$

where U_{field} is the electromagnetic field energy in the mode, ω is the eigenmode frequency, $\mathbf{k}$ is a generalized wave vector (e.g. Bloch wave vector, in periodic waveguides), and ξ is the separation. For the purposes of calculating the force, the derivative should be taken at fixed wave vector. However, once the force is calculated for a particular frequency, wave vector, and separation, the value is unique. Thus while in an experiment, the system is generally fixed at a given frequency (rather than wave vector, as in Equation 2), the value calculated in this manner is still correct. The eigenmode frequency at fixed separation can be calculated using the plane-wave expansion method, and the derivative taken numerically by calculating the shifted frequency at a shifted separation.

2. HIGH INDEX CONTRAST

As a protypical example of the type of effect we are interested in studying, we consider the optically-induced forces between parallel, high-index waveguides. When two parallel waveguides are brought close together, the modes of the waveguides couple and split in frequency. This splitting results in a force, which can be either attractive or repulsive depending which of the two split modes is excited. By controllably coupling into either the attractive or repulsive mode, the waveguides can be either pulled closer together or pushed further apart. The predicted effect should be observable under typical experimental conditions. For example, we estimate[2] that for suspended silicon waveguides with cross-sectional dimensions of 310x310 nm, 30 μm length and an input power of 100 mW, the deflection can be as large as 20 nm at the center of the waveguide. Intuitively, the force is "caused" by the polarization of the dielectric waveguides, which causes them to attract or repel. Alternatively, the force can be seen as a result of the eigenmode splitting, similar in spirit to the way in which splitting of electronic states gives rise to bonding and anti-bonding states in solids.

A typical geometry is shown in Figure 1(a). Figure 1(b) shows the calculated dispersion relation for modes with y-odd vector symmetry (electric field primarily in the y-direction for large separations). Frequency is plotted in dimensionless units $\nu a/c$, where $\nu = \omega/(2\pi)$. k is the magnitude of the wave vector, which is parallel to the waveguide axes. Note that $\nu a/c = a/\lambda$, where λ is the free-space wavelength. The upper left, shaded region of the dispersion relation indicates the light cone, in which there exist extended modes in air. Modes lying under the light cone are guided by the waveguides. The solid line indicates the dispersion relation of the waveguides for infinite separation; in this limit the waveguides do not couple, and the force is zero. The dashed and dotted lines show the dispersion relations for two decreased separations. As the waveguides are brought together, the original eigenmode splits into upper and lower branches. These correspond to anti-symmetric and symmetric combinations of the waveguide phases, as shown in the inset.

The force between the waveguides is shown in Figure 1(c). Note that excellent agreement is obtained between the Maxwell Stress Tensor method (solid curves) and the derivative expression (symbols). At larger separations ($d/a > 0.3$), the anti-symmetric mode gives a repulsive force and the symmetric force gives an attractive force. The magnitude of the force decreases with separation as the overlap between the waveguide modes decreases. At smaller separations, the anti-symmetric mode exhibits a strongly attractive force due to field enhancement inside the slit resulting from the high-index-contrast boundary conditions.[7] Left and bottom axes show the force per unit length (F/L) in dimensionless units, where P is the input power, as a function of distance. Right and bottom axes show physical values for a specific choice of parameters given in the caption.

The choice of a material with relatively high index ($n = 3.45$ for silicon at wavelengths near 1.55 μm) enhances the magnitude of the optical force. Intuitively, in the larger-separation, weak-coupling regime, overlap between waveguide modes causes either attraction or repulsion. For very low indices, the waveguide modes are much less weakly confined to the dielectric and extend further in the air. In the limit that $n \to 1$, the modes are completely

unconfined, and will not change with separation, giving no force. For very high indices on the other hand, the waveguide modes are strongly confined within the dielectric, and will not overlap one another. In the limit that $n \to \infty$, the modes again decouple. Thus for a given waveguide geometry and separation, we expect that the force as a function of index will peak. While it is possible to optimize n for a given geometry, the limited choice of viable materials systems/indices amenable to microfabrication instead suggest the further optimization of design parameters at fixed index. Indeed, our preliminary results show that significant forces can also be obtained for silica(fiber)/air index contrasts as well.

3. HIGH-Q ENHANCEMENT

Having demonstrated that attractive and repulsive forces result from the coupling of waveguide modes in parallel strip waveguides, we can extend the discussion to a similar phenomenon occuring in coupled, high-Q microspheres. Whispering gallery mode (WGM) resonances in microspheres are known to have extremely high experimental values of cavity quality factor Q,[8,9] yielding large optical energy enhancements inside the sphere relative to the input power. For certain choices of the angular mode numbers, a WGM resembles the mode of a circular strip waveguide lying along the sphere equator– the mode is highly confined to the region near the equator and near the surface of the sphere.[10] For two closely-separated microspheres, coupling between the modes of the spheres can give an attractive or repulsive force in a similar way to the parallel waveguides above.

We focus on WGM modes with TE-polarization ($\vec{E}$) perpendicular to the radial direction, with angular mode number l equal to the azimuthal mode number m. For large mode numbers, direct calculation of the WGM modes becomes prohibitive. Instead, we calculate the shift in the mode frequency due to coupling via perturbative methods and find the force from Equation 2. Here, the derivative is taken at fixed mode number rather than fixed wavevector $\mathbf{k}$. Further details on the calculation method and derivation of the derivative expression are given in our previous paper.[3]

Results for the force are shown in Figure 2. On the left and bottom axes, force is shown as a function of distance in dimensionless units, where λ is the free-space wavelength and U is the total electromagnetic field energy. For the antisymmetric mode, the force is repulsive, whereas for the symmetric mode, the force is attractive. Force decreases with distance, as the modal overlap decreases. In addition, the force decreases with increasing angular mode number between $l = m = 111$ and $l = m = 184$. This effect is due to increasing radial confinement.

The key to high-Q enhancement of the optical force is that the total electromagnetic field energy U for fixed input power increases directly with Q: $U = PQ/\omega$. The total force scales linearly with U, and hence Q. Assuming an input power of 1 mW and $Q = 10^8$, we obtain the values shown on the top and right axes of the graph. It can be seen that forces on the order of 100 nN are obtained for separations on the order of 100 nm.

.

4. SLOW LIGHT ENHANCEMENT

A third mechanism for the enhancement of optical forces in guided-wave devices is the use of slow-light structures.[1] Above, we have seen that optical forces are directly proportional to the electromagnetic field energy in the guided-wave mode of interest. Under conditions of fixed power input to a guided-wave mode, the electromagnetic field energy U scales as the input power over the group velocity. Consequently, reducing the group velocity of a mode increases the optical force at fixed input power.

In previous work,[1] we have analyzed in detail the slow-light waveguide shown in Figure 3(a). Light propagates in the air gap between two multilayer films, parallel to the film layers. Figure 3(b) shows the dispersion relation for the fundamental mode for the specific parameter choices given in the caption. As the films are brought closer together (increasing a/d), the fundamental mode moves up in frequency within a band gap in the extended modes of the bulk film. For constant operating frequency, the group velocity decreases until the mode is cutoff; e.g. there is no longer a fundamental guided mode at that frequency. The optical force will be maximized in the slow-light region before cutoff. To optimize the optical force, we want to ensure maximal confinement of the guided mode to the air region between the films. This is achieved by choosing the layer thicknesses to satisfy

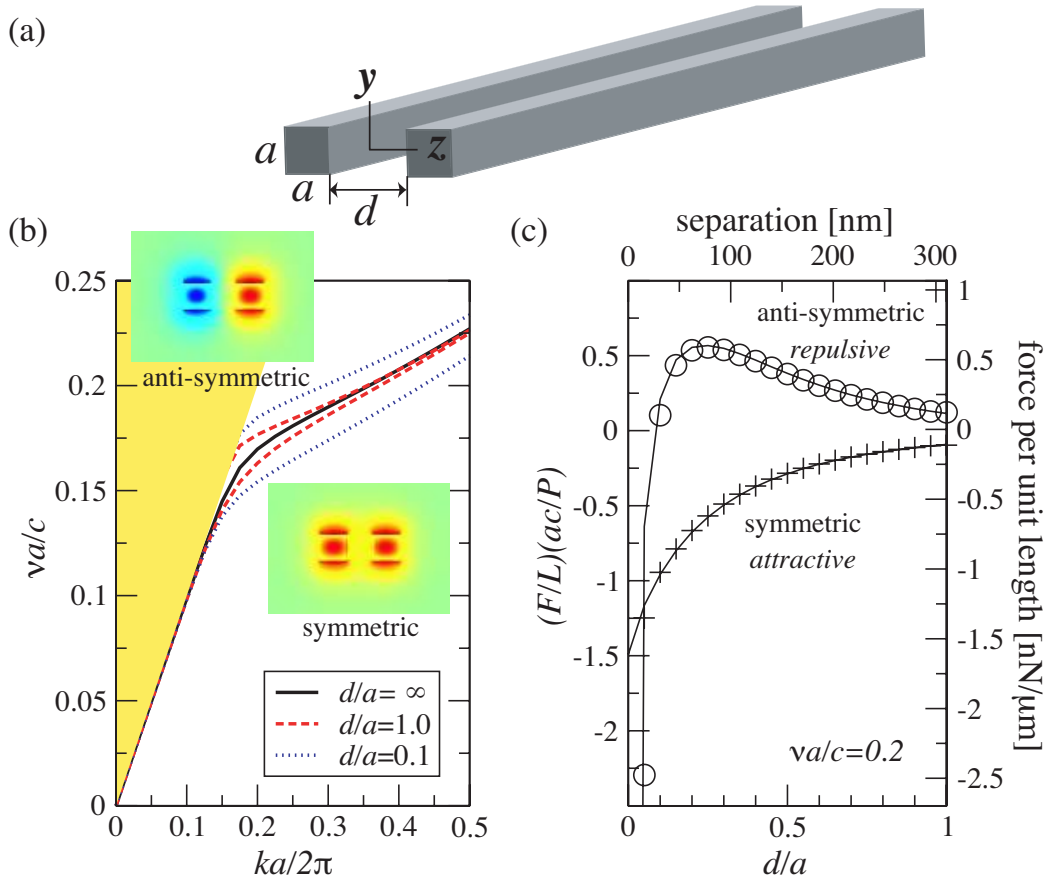

Figure 1. (a) Parallel, high-index ($n = 3.45$; silicon) waveguides. (b) Dispersion relation for varying waveguide separations for modes with y-odd vector symmetry (electric field primarily in the y-direction in the isolated waveguide). Insets show E_y for anti-symmetric and symmetric modes with $d/a = 1.0$. Blue/red indicates positive/negative values. (c) Normalized force per unit length as a function of separation for a frequency $\nu a/c = 0.2$. Left and bottom axes are in dimensionless units; tight and top units show physical units for $P = 100$ mW, $\lambda = 1.55\,\mu$m, and $a = 310$ nm. Solid curves are calculated using the stress tensor method (Equation 1) and symbols are calculated from the eigenmode frequency derivative expression (Equation 2).

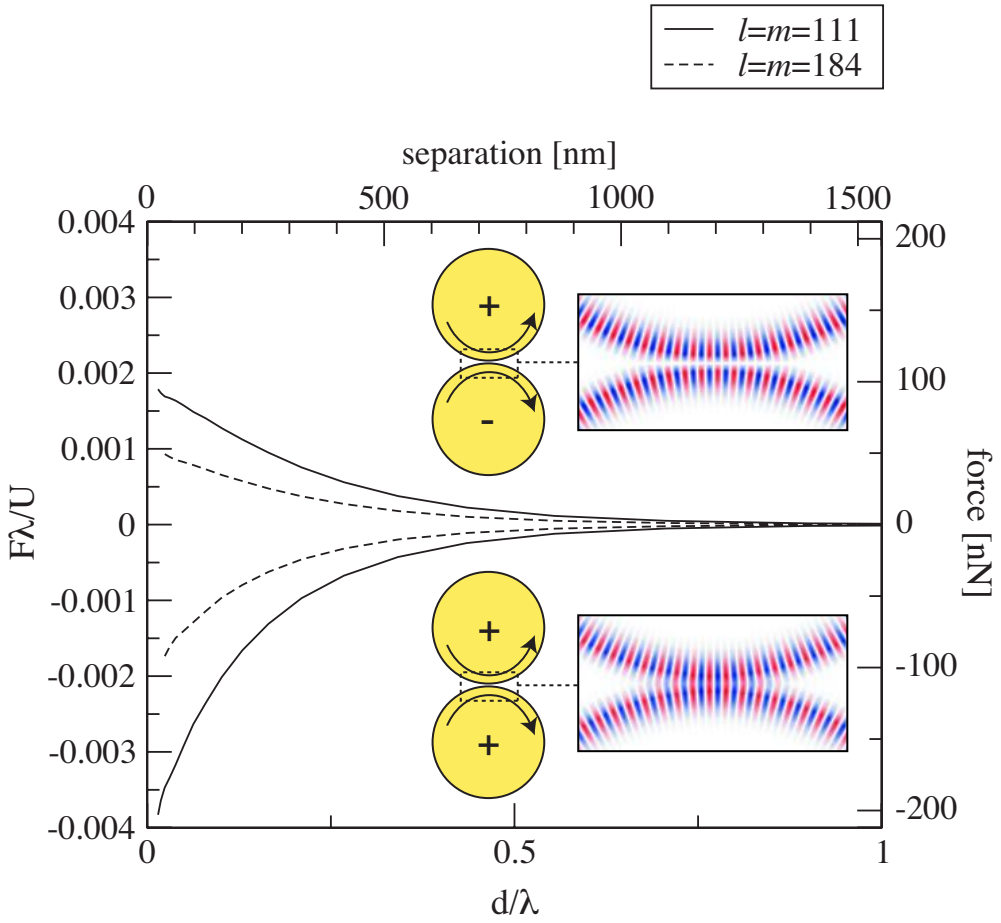

Figure 2. Force as a function of separation between two microspheres with excited whispering-gallery modes. d is the edge-to-edge separation, λ is the free-space wvelength, and U is the total electromagnetic field energy. Insets show the symmetry of the repulsive ($F > 0$) and attractive ($F < 0$) modes. Red/blue values respresent positive/negative values of the electric field perpendicular to the page. Right and top axes display force vs. distance in physical units for input power $P = 1$ mW and microsphere quality factor $Q = 10^8$.

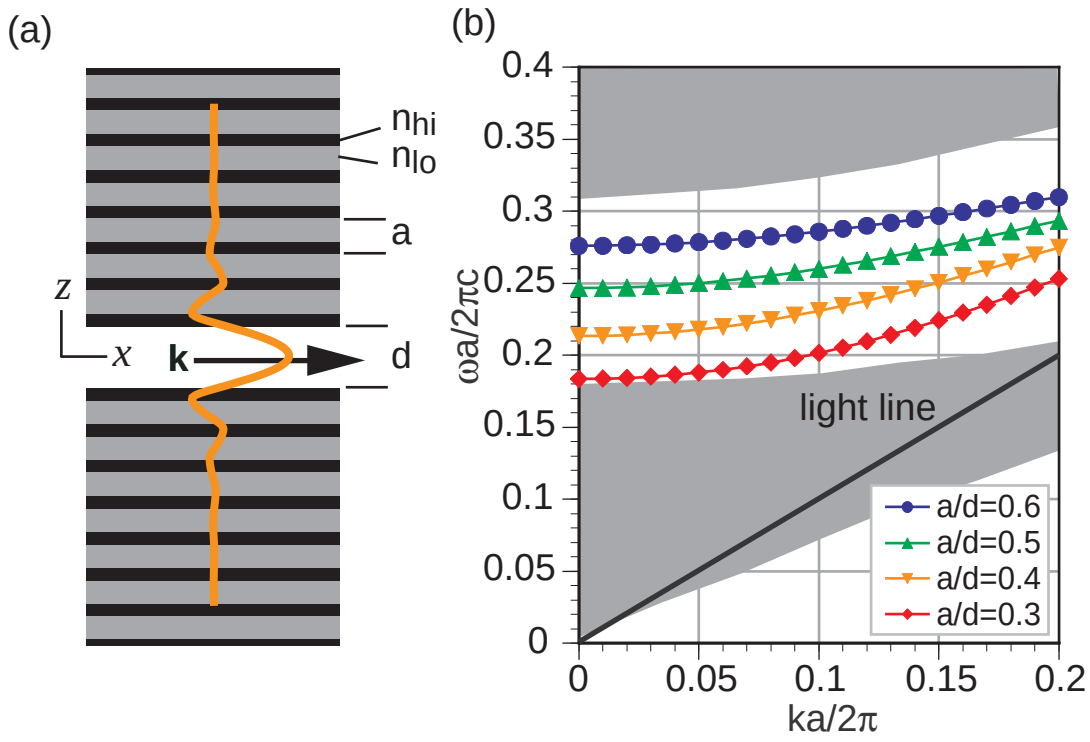

Figure 3. (a) Slow-light waveguide made up of two multilayer films: two multilayer films of period a are separated by a distance d; each film is made up of layers with alternating refractive indices $n_{\rm hi} = 3.45$ and $n_{\rm lo} = 1.45$. Light propagates parallel to the films with wave vector $\mathbf{k}$. The field profile of the fundamental mode is superimposed on the structure. (b) Dispersion relation for the waveguide of (a) for varying distances between the films for modes with $\mathbf{E} \parallel \hat{y}$. Layer thicknesses are chosen to satisfy the quarter-wave condition. Shaded grey regions indicate bulk modes of the multilayer film, and symbols indicate the dispersion relation for the fundamental mode of the waveguide for varying values of a/d.

the quarter-wave condition, and moreover by fixing $a/d = 0.45$, as shown.[1] Supposing that we want to achieve a large force at a particular separation d_o, we set $a = 0.45 d_o$ and moreover choose the operating frequency such that the group velocity of the mode is zero for this separation.

Figure 4(a) shows the scaled group velocity, v_g/c (where c is the speed of light in vacuum) and dimensionless force $Fd_o/U_{\rm field}$. As the distance between the plates is decreased (decreasing d/d_o), the group velocity decreases to zero and the force increases. Note that this force is the optical force at *fixed electromagnetic field energy.* The increase in force at smaller distances can be explained by the increased localization of the mode in the air region near cutoff. We now consider the force at *constant input power,* which more closely approximates experimental conditions. In this case, the scaling of the field energy as $1/v_g$ leads to a divergence in the optical force as the distance is decreased, as shown in Figure 4(b). In practice, due to the simultaneous divergence of the absorption loss at mode cutoff, this feature should show up as a rounded-off peak. Figure 4(c) suggests a method of adiabatically tapering the waveguide to ensure nearly constant input power. The lower film is flat, whereas the upper film is deposited on the surface of a sphere. For sphere radii much larger than the film separation, a given fractional change in the center-to-center film separation produces a far smaller fractional change in the width of the input and output tapers.

The slow-light enhancement mechanism discussed here relies on very general scaling arguments, and so is not unique to the particular waveguide structure studied here. As a result, it should be applicable to a variety of slow-light photonic-crystal/grating designs.

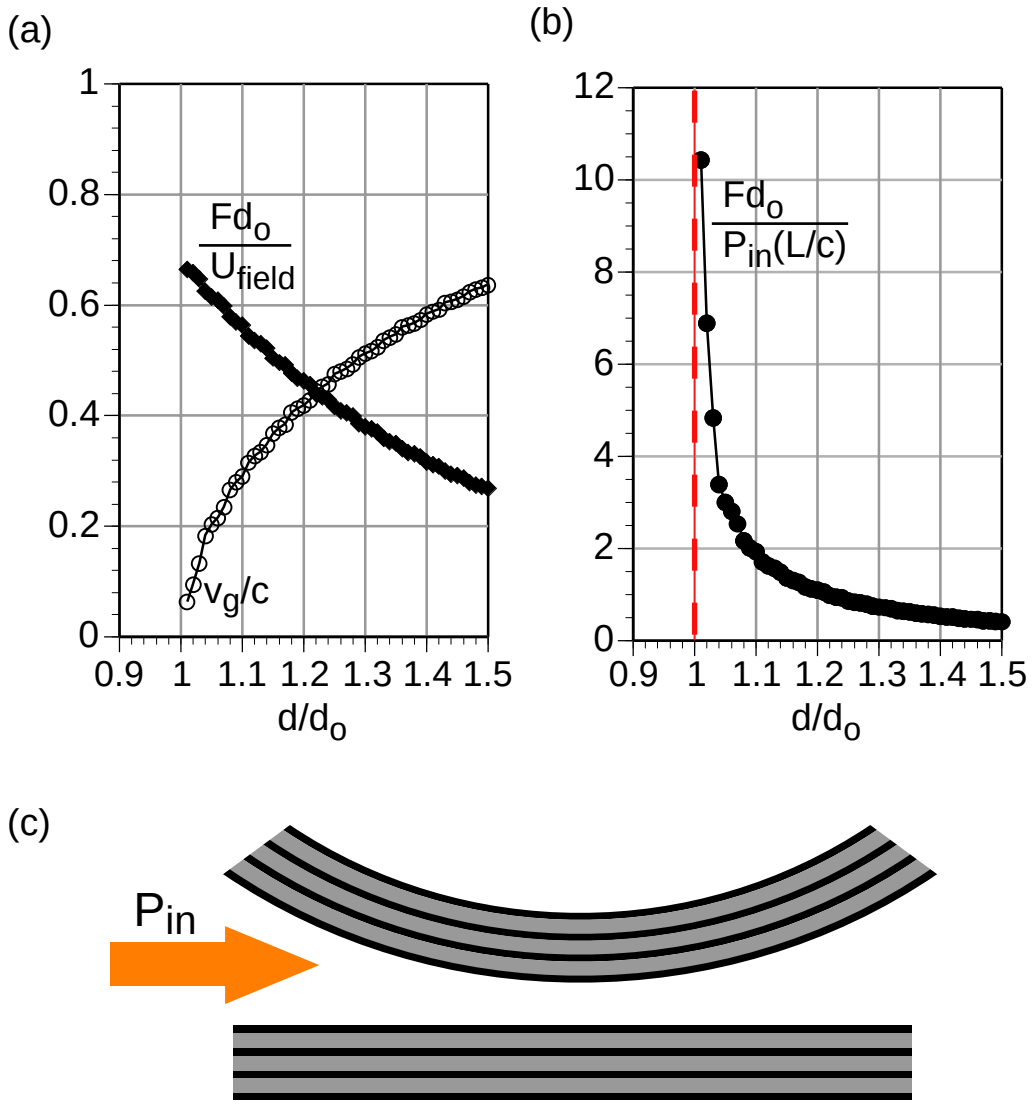

Figure 4. (a) Force as a function of separation between the films at fixed frequency and field energy. (b) Force as a function of separation at fixed frequency and input power. (c) Adiabatic tapering scheme for achieving constant power input over a range of separations.

5. CONCLUSION

We have summarized our work on optical forces in the context of integrated microphotonics, with an emphasis on mechanisms for enhancing the optical fields and consequently the forces. We are hopeful that these methods will allow the observation of significant mechanical displacements in our ongoing experiments and lead to the possibility of device reconfiguration using light signals.

REFERENCES

1. M. L. Povinelli, M. Ibanescu, S. G. Johnson, and J. D. Joannopoulos, "Slow-light enhancement of radiation pressure in an omnidirectional-reflector waveguide," *Appl. Phys. Lett.* **85**(9), pp. 1466–1468, 2004.
2. M. L. Povinelli, M. Loncar, M. Ibanescu, E. J. Smythe, S. G. Johnson, F. Capasso, and J. D. Joannopoulos, "Evanescent-wave bonding between optical waveguides," *Opt. Lett.* **30**, pp. 3042–3044, Nov. 2005.
3. M. L. Povinelli, S. G. Johnson, M. Lončar, M. Ibanescu, E. J. Smythe, F. Capasso, and J. D. Joannopoulos, "High-Q enhancement of attractive and repulsive optical forces between whispering-gallery-mode resonators," *Opt. Express* **13**, pp. 8286–8295, Oct. 2005.
4. J. D. Jackson, *Classical Electrodynamics*, Wiley, New York, third ed., 1998.
5. M. I. Antonoyiannakis and J. B. Pendry, "Electromagnetic forces in photonic crystals," *Phys. Rev. B* **60**, pp. 2363–2374, July 1999.
6. S. G. Johnson and J. D. Joannopoulos, "Block-iterative frequency-domain methods for Maxwell's equations in a planewave basis," *Opt. Express* **8**, pp. 173–190, Jan. 2001.
7. V. R. Almeida, Q. Xu, C. A. Barrios, and M. Lipson *Opt. Lett.* **29**, p. 1209, 2004.
8. S. M. Spillane, T. J. Kippenberg, and K. J. Vahala, "Ultralow-threshold raman laser using a spherical dielectric microcavity," *Nature* **415**, pp. 621–623, February 2002.
9. S. M. Spillane, T. J. Kippenberg, O. J. Painter, and K. J. Vahala, "Ideality in a fiber-taper-coupled microresonator system for application to cavity quantum electrodynamics," *Physical Review Letters* **91**, p. 043902, July 2003.
10. B. R. Johnson, "Theory of morphology-dependent resonances: shape resonances and width formulas," *J. Opt. Soc. Am. A* **10**, pp. 343–352, 1993.